Supplementary Information for

TQPHEN (*N,N,N′,N′*-tetrakis(2-quinolylmethyl)-1,2-phenylenediamine) derivatives as highly selective fluorescent probes for Cd^{2+}

Yuji Mikata,[a,b,*] Asako Kizu[b] and Hideo Konno[c]

[a]*KYOUSEI Science Center and* [b]*Department of Chemistry, Faculty of Science, Nara Women's University, Nara 630-8506, Japan and* [c]*National Institute of Advanced Industrial Science and Technology (AIST), 1-1-1 Higashi, Tsukuba, Ibaraki 305-8565, Japan*

Table S1 Crystallographic data for $[Cd(TQPHEN)](ClO_4)_2 \cdot CH_3OH$ and $[Zn(TQPHEN)](ClO_4)_2 \cdot CH_3OH$

	$[Cd(TQPHEN)](ClO_4)_2 \cdot CH_3OH$	$[Zn(TQPHEN)](ClO_4)_2 \cdot CH_3OH$
Formula	$C_{47}H_{40}CdCl_2N_6O_9$	$C_{47}H_{40}Cl_2N_6O_9Zn$
FW	1016.18	969.15
Crystal system	triclinic	triclinic
Space group	*P*-1	*P*-1
a, Å	11.703(6)	11.636(2)
b, Å	12.445(7)	12.245(2)
c, Å	16.362(8)	16.549(3)
α, deg	102.022(6)	101.2169(13)
β, deg	92.925(4)	94.8706(12)
γ, deg	111.880(7)	113.2015(12)
V, Å^3	2135(2)	2091.5(6)
Z	2	2
D_{calc}, g cm^{-3}	1.581	1.539
μ, mm^{-1}	0.7043	0.7832
$2\theta_{max}$, deg	55	55
temp, K	153	153
no. reflns collected	20959	20682
no. reflns used	9565	9375
no. of params	595	595
R_{int}	0.0188	0.0175
Final *R*1 ($I > 2\sigma(I)$)[a]	0.0391	0.0412
*wR*2 (all data)[b]	0.1029	0.1143
GOF	1.059	1.051

[a] $R1 = \Sigma||F_o| - |F_c||/\Sigma|F_o|$. [b] $wR2 = [\Sigma w[(F_o^2 - F_c^2)^2]/\Sigma[w(F_o^2)^2]]^{1/2}$.

Table S2 Interatomic distances (Å) and angles (°) for $[Cd(TQPHEN)](ClO_4)_2 \cdot CH_3OH$ and $[Zn(TQPHEN)](ClO_4)_2 \cdot CH_3OH$

	$[Cd(TQPHEN)](ClO_4)_2 \cdot CH_3OH$	$[Zn(TQPHEN)](ClO_4)_2 \cdot CH_3OH$
M-N1	2.377(3)	2.1915(19)
M-N2	2.393(3)	2.1993(17)
M-N3	2.2863(18)	2.1237(14)
M-N4	2.461(3)	2.3207(18)
M-N5	2.259(2)	2.1104(17)
M-N6	2.536(3)	2.5606(18)
N1-M-N2	73.98(7)	78.58(6)
N1-M-N3	72.22(9)	76.74(7)
N1-M-N4	74.57(8)	78.80(7)
N1-M-N5	142.96(8)	152.57(7)
N1-M-N6	90.68(8)	92.75(7)
N2-M-N3	141.21(9)	148.74(7)
N2-M-N4	90.33(8)	94.93(7)
N2-M-N5	72.09(8)	76.10(7)
N2-M-N6	73.58(8)	76.10(7)
N3-M-N4	98.47(8)	98.76(6)
N3-M-N5	144.61(9)	130.62(8)
N3-M-N6	88.29(7)	86.20(6)
N4-M-N5	91.13(8)	92.98(7)
N4-M-N6	160.82(9)	168.85(8)
N5-M-N6	93.65(8)	91.28(7)
M-N3-C(4)	166.84(12)	167.02(10)
M-N4-C(4)	143.34(11)	143.35(9)
M-N5-C(4)	169.19(13)	164.47(11)
M-N6-C(4)	139.02(12)	136.23(10)

Table S3 Interatomic distances (Å) and angles (°) for zinc and cadmium complexes for TQEN, TQDACH and TQPHEN

	TQEN	TQDACH	TQPHEN
Zn-N1	2.1497(14)	2.2043(19)	2.1915(19)
Zn-N2	2.1681(14)	2.1804(16)	2.1993(17)
Zn-N3	2.1543(14)	2.1421(14)	2.1237(14)
Zn-N4	2.4007(15)	2.2887(18)	2.3207(18)
Zn-N5	2.1271(14)	2.1269(17)	2.1104(17)
Zn-N6	2.3711(15)	2.4848(19)	2.5606(18)
Zn-N3-C(4)	159.48(9)	168.46(10)	167.02(10)
Zn-N4-C(4)	165.67(9)	152.57(10)	143.35(9)
Zn-N5-C(4)	163.95(9)	166.67(10)	164.47(11)
Zn-N6-C(4)	167.32(10)	139.56(10)	136.23(10)
Cd-N1	2.400(3)	2.386(4)	2.377(3)
Cd-N2	2.377(3)		2.393(3)
Cd-N3	2.354(3)	2.289(4)	2.2863(18)
Cd-N4	2.370(2)	2.472(3)	2.461(3)
Cd-N5	2.376(3)		2.259(2)
Cd-N6	2.435(2)		2.536(3)
Cd-N3-C(4)	162.57(11)	164.75(18)	166.84(12)
Cd-N4-C(4)	164.21(15)	140.48(14)	143.34(11)
Cd-N5-C(4)	165.98(13)		169.19(13)
Cd-N6-C(4)	147.24(13)		139.02(12)

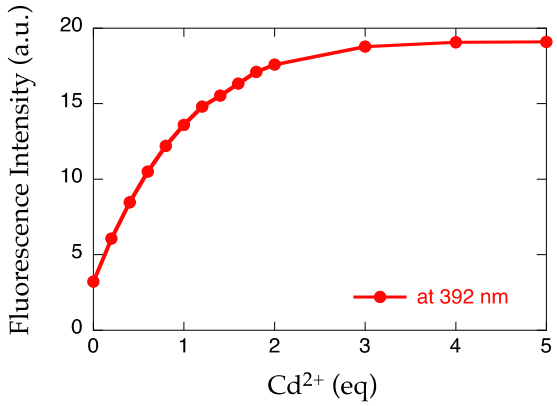

Fig. S1 Plot for fluorescence intensity changes at 392 nm in the Cd^{2+} titration of 34 μM TQPHEN in DMF-H_2O (1:1) at 25 °C (λ_{ex} = 317 nm).

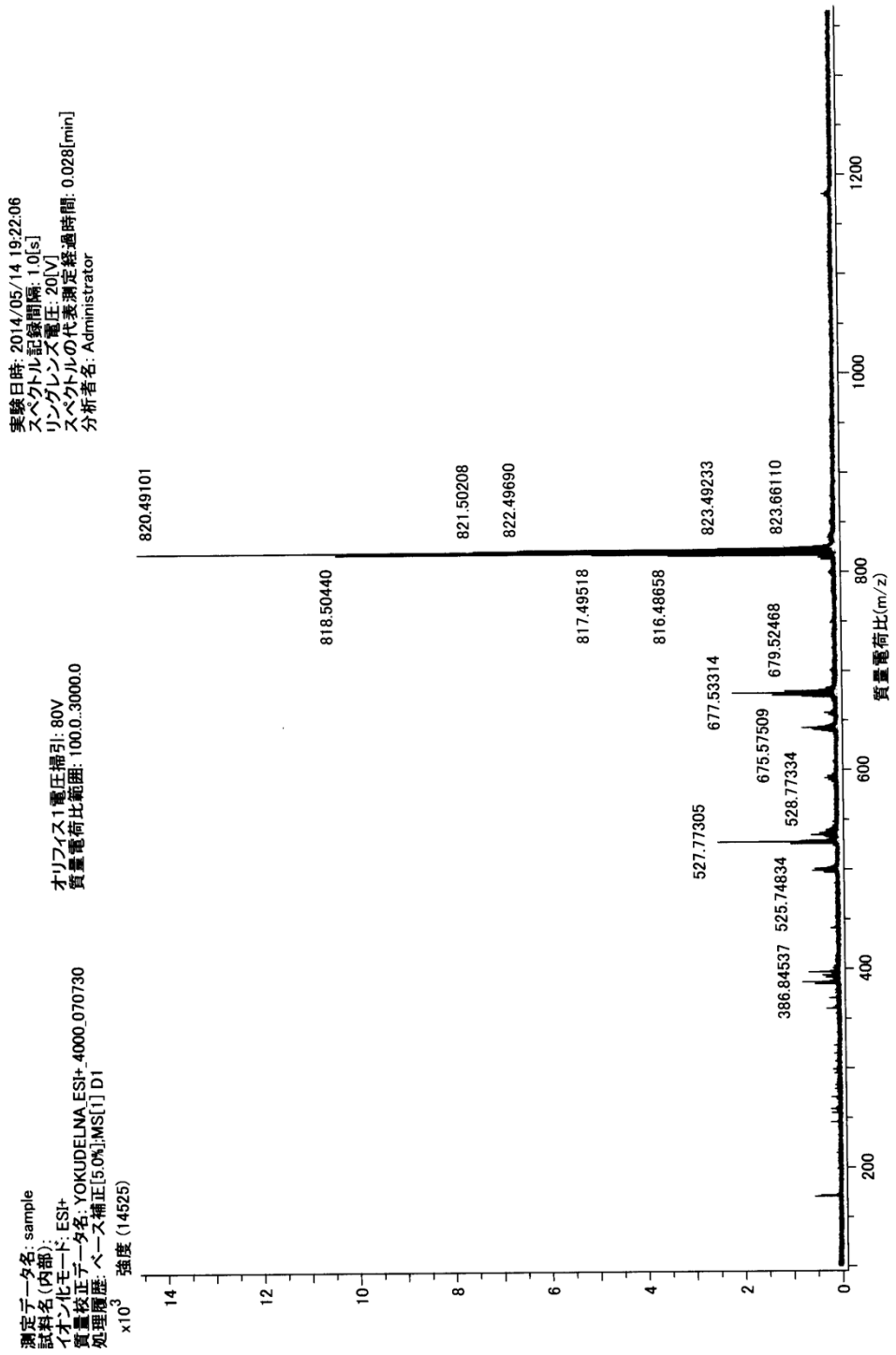

Fig. S2 ESI-MS spectrum for TQPHEN in the presence of 3 equiv. of Cd^{2+} in MeOH.

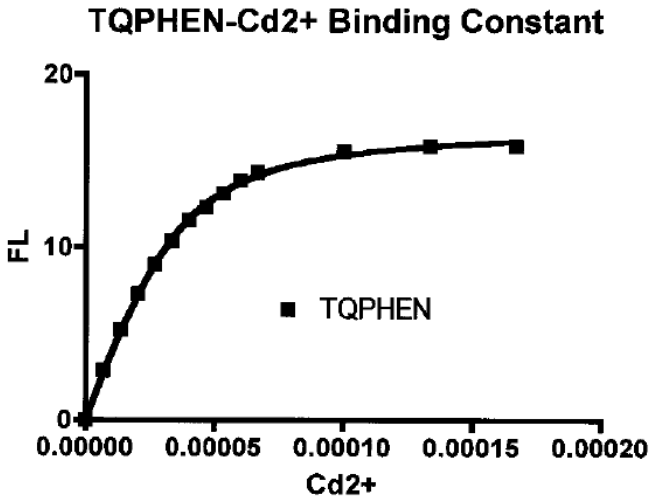

Cd2+	TQPHEN2
0.000000	0.0000
6.666700e-06	2.8626
1.333300e-05	5.2479
2.000000e-05	7.2973
2.666700e-05	8.9903
3.333300e-05	10.3740
4.000000e-05	11.5940
4.666700e-05	12.3350
0.000053	13.1170
0.000060	13.8940
0.000067	14.3750
0.000100	15.5680
0.000133	15.8580
0.000167	15.8750

	TQPHEN2
Best-fit values	
BMAX	17.05
KD	7.7565e-006
L0	3.4000e-005
Std. Error	
BMAX	0.1645
KD	4.6957e-007
95% Confidence Intervals	
BMAX	16.69 to 17.41
KD	6.7333e-006 to 8.7797e-006
Goodness of Fit	
Degrees of Freedom	12
R squared	0.9989
Absolute Sum of Squares	0.3493
Sy.x	0.1706
Constraints	
L0	L0 = 3.4000e-005
Data	
Number of X values	14
Number of Y replicates	1
Total number of values	14
Number of missing values	0

Fig. S3 Estimation of dissociation constant of TQPHEN with Cd^{2+} in DMF-H_2O (1:1).

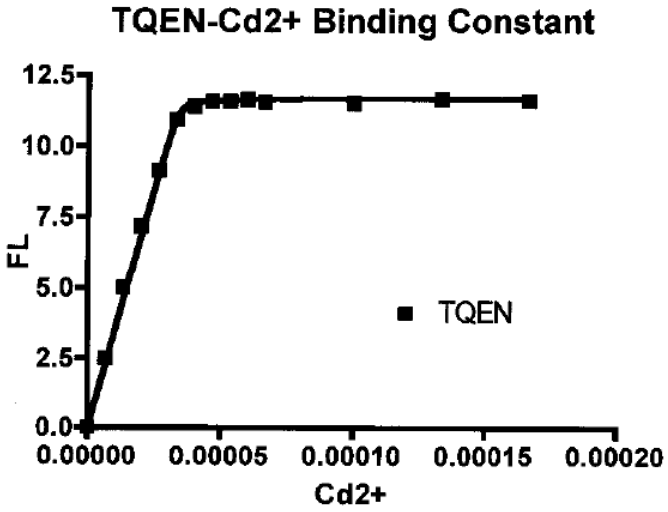

Cd2+	TQEN
0.000000	0.0000
6.666700e-06	2.5172
1.333300e-05	5.0132
2.000000e-05	7.1648
2.666700e-05	9.1530
3.333300e-05	10.9280
4.000000e-05	11.3930
4.666700e-05	11.5840
0.000053	11.5840
0.000060	11.6400
0.000067	11.5680
0.000100	11.5210
0.000133	11.6660
0.000167	11.5980

	TQEN
Best-fit values	
BMAX	11.68
KD	9.3289e-008
L0	3.4000e-005
Std. Error	
BMAX	0.08292
KD	6.7687e-008
95% Confidence Intervals	
BMAX	11.50 to 11.86
KD	-5.4202e-008 to 2.4078e-007
Goodness of Fit	
Degrees of Freedom	12
R squared	0.9978
Absolute Sum of Squares	0.4359
Sy.x	0.1906
Constraints	
L0	L0 = 3.4000e-005
Data	
Number of X values	14
Number of Y replicates	1
Total number of values	14
Number of missing values	0

Fig. S4 Estimation of dissociation constant of TQEN with Cd^{2+} in DMF-H_2O (1:1).

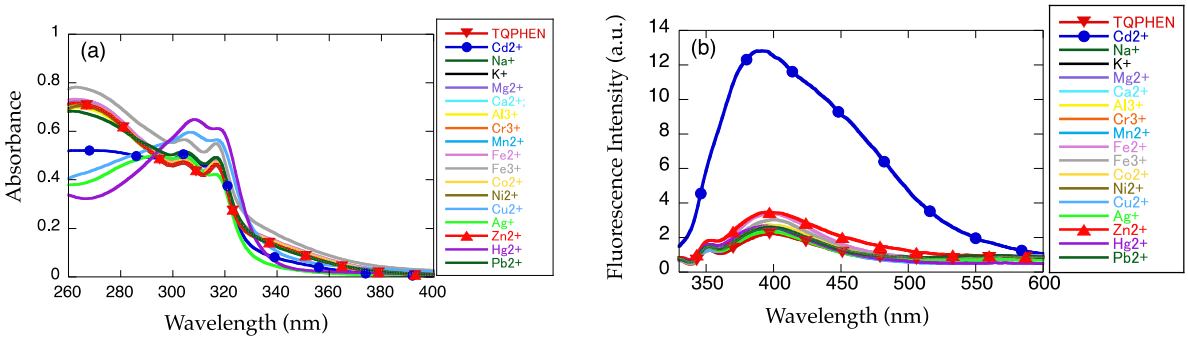

Fig. S5 (a) Absorbance and (b) fluorescence spectra of 34 μM TQPHEN in the presence of 1 equiv. of various metal ions in DMF-H_2O (1:1) at 25 °C (λ_{ex} = 317 nm).

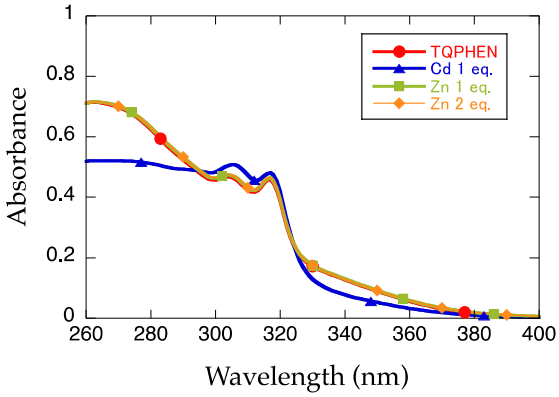

Fig. S6 Absorbance spectra of 34 μM TQPHEN in DMF-H_2O (1:1) at 25 °C in the presence of Cd^{2+} or Zn^{2+}.

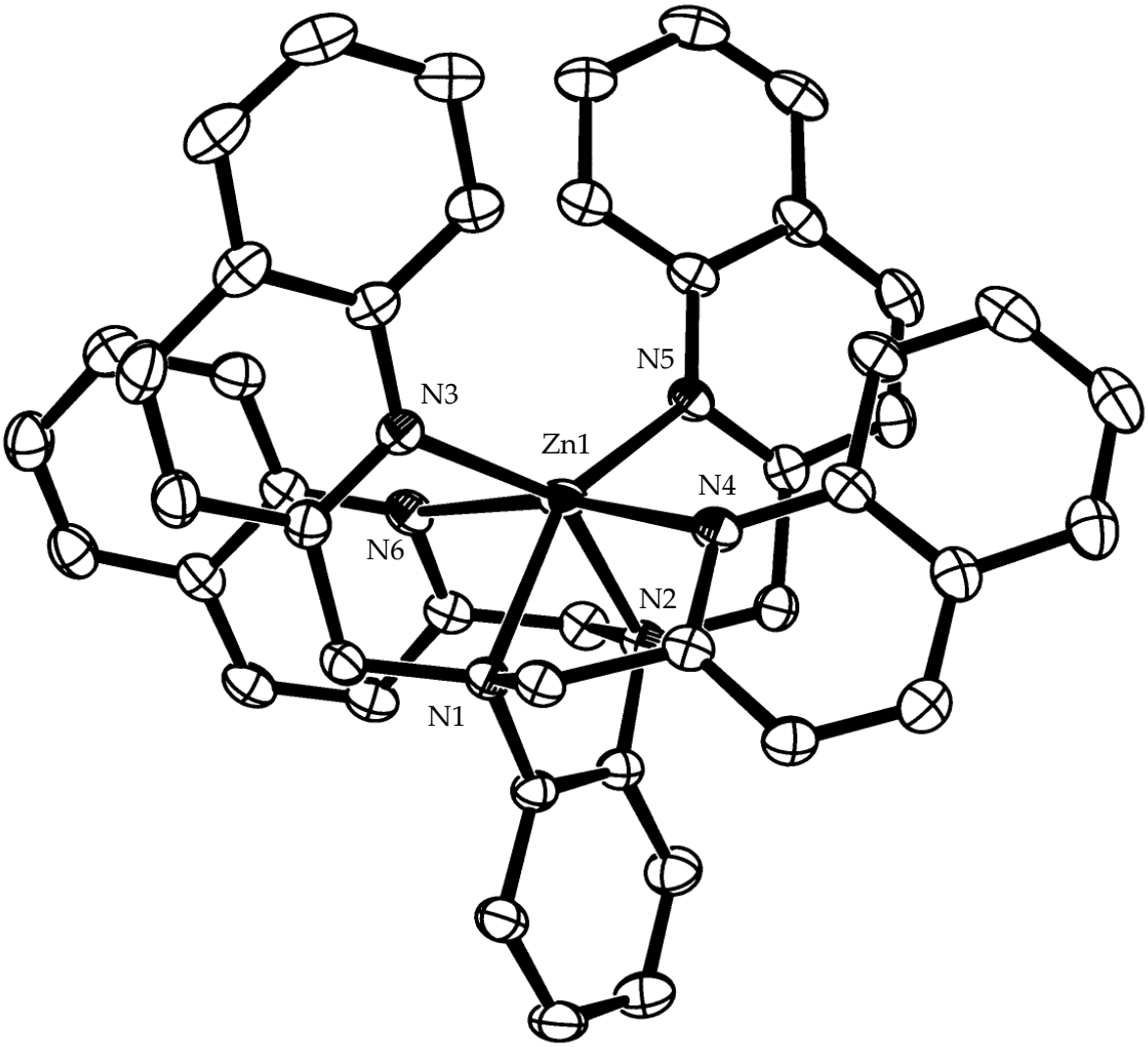

Fig. S7 ORTEP plot for cationic portion of $[Zn(TQPHEN)](ClO_4)_2$ with 50% thermal ellipsoids. Hydrogen atoms are omitted for clarity.

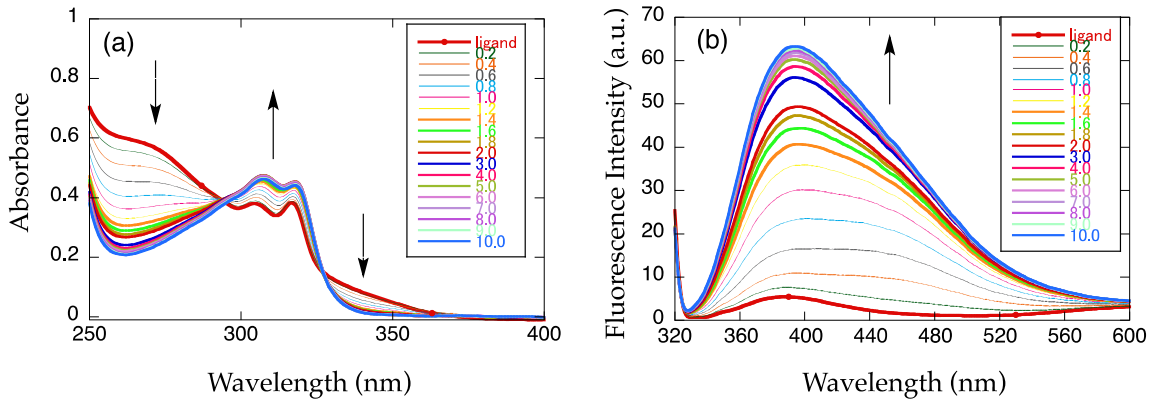

Fig. S8 Zn^{2+} titration profile for 34 μM TQPHEN in $CHCl_3$-CH_3OH (1:4) at 25 °C. (a) Absorbance changes. (b) Fluorescence changes (λ_{ex} = 317 nm).

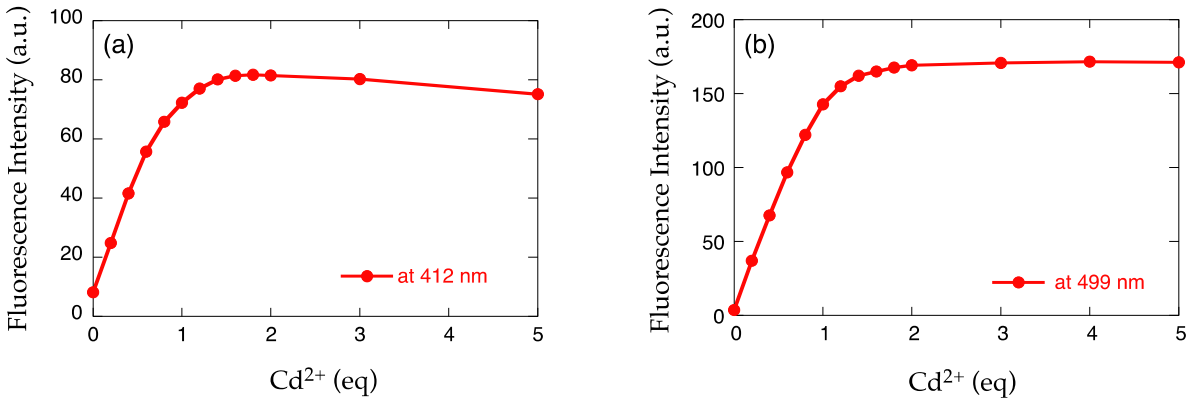

Fig. S9 Plot for fluorescence intensity changes of 34 μM (a) 6-MeOTQPHEN (at 412 nm) and (b) TriMeOTQPHEN (at 499 nm) in the Cd^{2+} titration of in DMF-H_2O (1:1) at 25 °C (λ_{ex} = 332 nm).

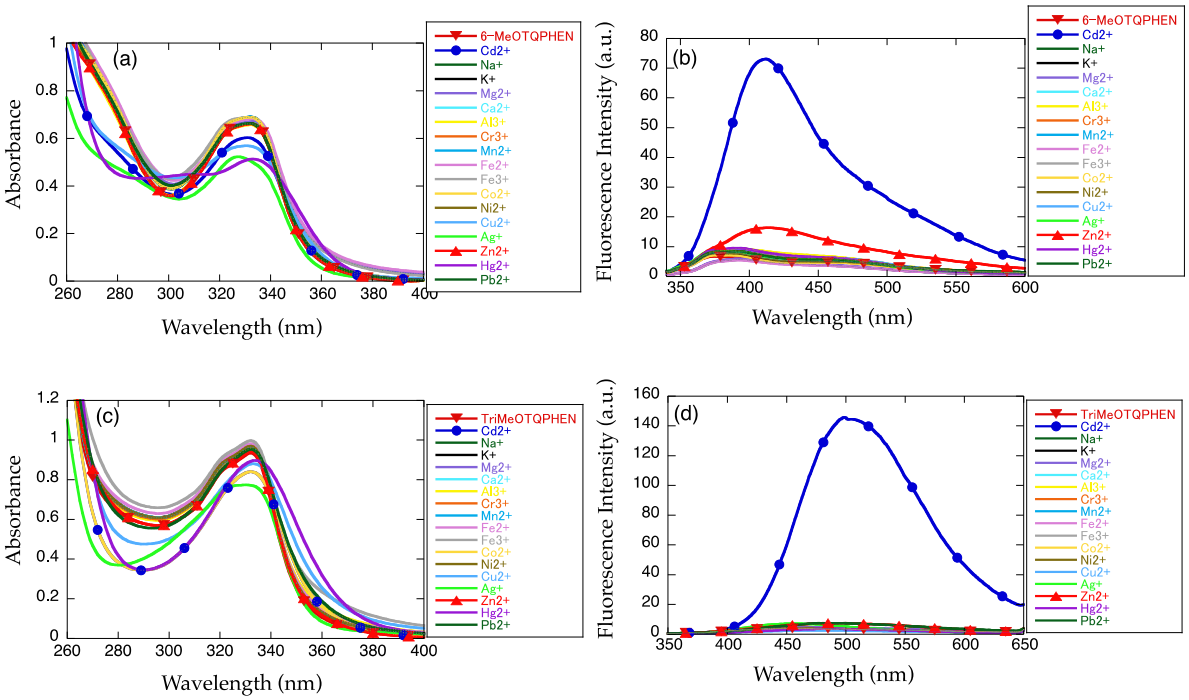

Fig. S10 (a, c) Absorbance and (b, d) fluorescence spectra of 34 μM (a, b) 6-MeOTQPHEN and (c, d) TriMeOTQPHEN in the presence of 1 equiv. of various metal ions in DMF-H_2O (1:1) at 25 °C (λ_{ex} = 332 nm).

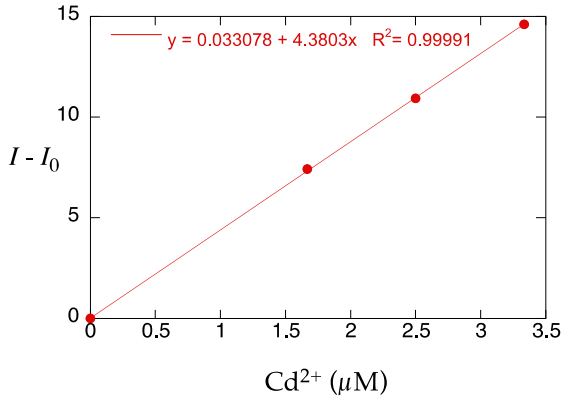

Fig. S11 Estimation of LOD (limit of detection) for Cd^{2+} with TriMeOTQPHEN in DMF-H_2O (1:1). The 3σ value (σ corresponds to standard deviation from 7 measurements) of blank solution (34 μM TriMeOTQPHEN) is 0.0469 in fluorescence intensity unit, which corresponds to 10.7 nM from the slope of the liner dynamic fluorescence intensity plot (*k*) shown above (LOD = 3σ/*k*).

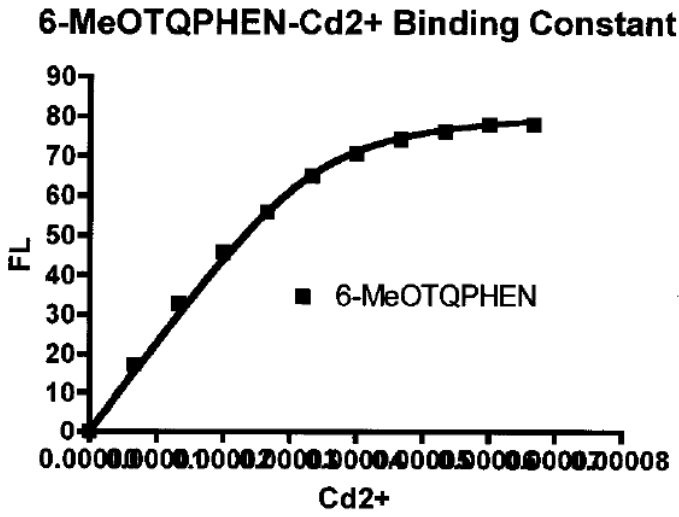

Cd2+	6-MeOTQPHEN
0.000000	0.0000
6.666700e-06	17.1910
1.333300e-05	32.9230
2.000000e-05	45.7630
2.666700e-05	55.9350
3.333300e-05	65.1530
4.000000e-05	70.6250
4.666700e-05	74.1980
0.000053	76.4020
0.000060	78.0070
0.000067	78.0640

	6-MeOTQPHEN
Best-fit values	
BMAX	82.87
KD	1.7464e-006
L0	3.4000e-005
Std. Error	
BMAX	1.983
KD	5.1481e-007
95% Confidence Intervals	
BMAX	78.38 to 87.35
KD	5.8190e-007 to 2.9109e-006
Goodness of Fit	
Degrees of Freedom	9
R squared	0.9977
Absolute Sum of Squares	16.59
Sy.x	1.358
Constraints	
L0	L0 = 3.4000e-005
Data	
Number of X values	11
Number of Y replicates	1
Total number of values	11
Number of missing values	0

Fig. S12 Estimation of dissociation constant of 6-MeOTQPHEN with Cd^{2+} in DMF-H_2O (1:1).

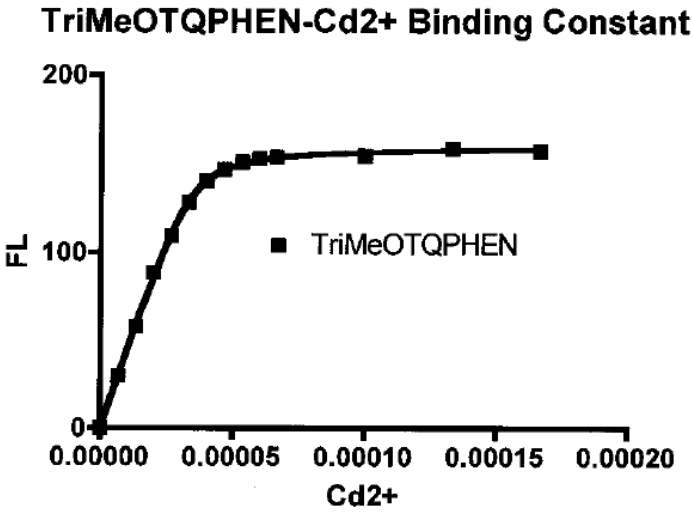

Cd2+	TriMeOTQPHEN
0.000000	0.0000
6.666700e-06	29.7250
1.333300e-05	57.9770
2.000000e-05	88.4120
2.666700e-05	109.3700
3.333300e-05	128.1200
4.000000e-05	140.4600
4.666700e-05	146.7700
0.000053	150.5400
0.000060	153.0800
0.000067	153.6700
0.000100	154.3200
0.000133	158.2400
0.000167	157.0100

	TriMeOTQPHEN
Best-fit values	
BMAX	159.4
KD	1.3592e-006
L0	3.4000e-005
Std. Error	
BMAX	0.7171
KD	1.0657e-007
95% Confidence Intervals	
BMAX	157.8 to 161.0
KD	1.1270e-006 to 1.5914e-006
Goodness of Fit	
Degrees of Freedom	12
R squared	0.9996
Absolute Sum of Squares	15.00
Sy.x	1.118
Constraints	
L0	L0 = 3.4000e-005
Data	
Number of X values	14
Number of Y replicates	1
Total number of values	14
Number of missing values	0

Fig. S13 Estimation of dissociation constant of TriMeOTQPHEN with Cd^{2+} in DMF-H_2O (1:1).

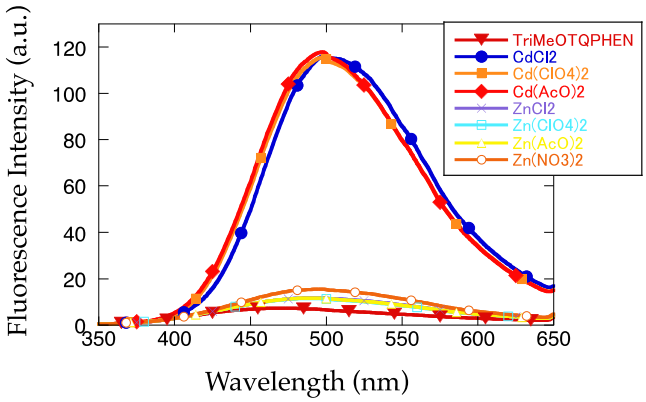

Fig. S14 Fluorescence spectra of 34 μM TriMeOTQPHEN in the presence of 1 equiv. of $CdCl_2$, $Cd(ClO_4)_2$, $Cd(AcO)_2$, $ZnCl_2$, $Zn(ClO_4)_2$, $Zn(AcO)_2$ and $Zn(NO_3)_2$ in DMF-H_2O (1:1) at 25 °C (λ_{ex} = 332 nm).

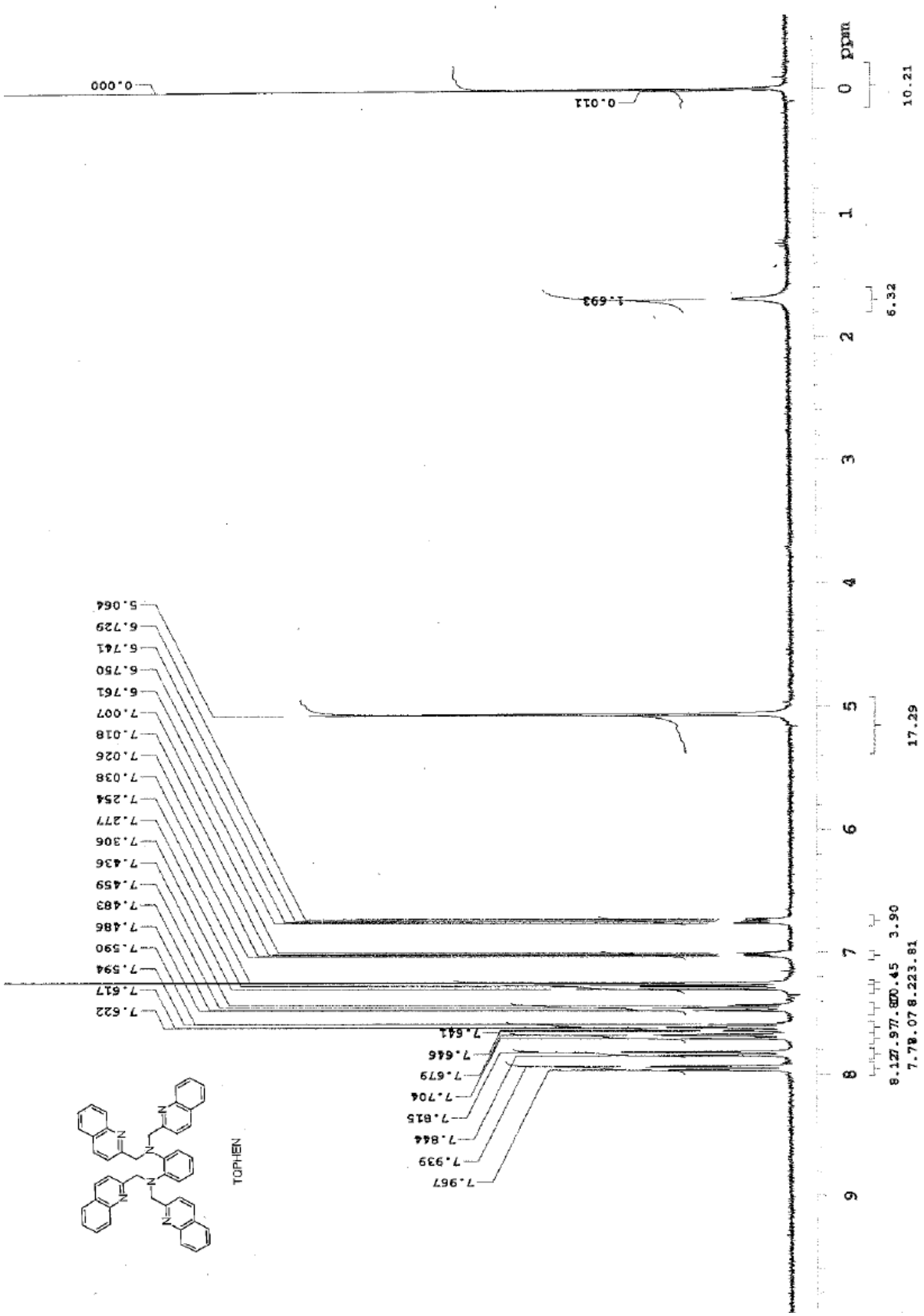

Fig. S15 ^{1}H NMR spectrum of TQPHEN in $CDCl_3$.

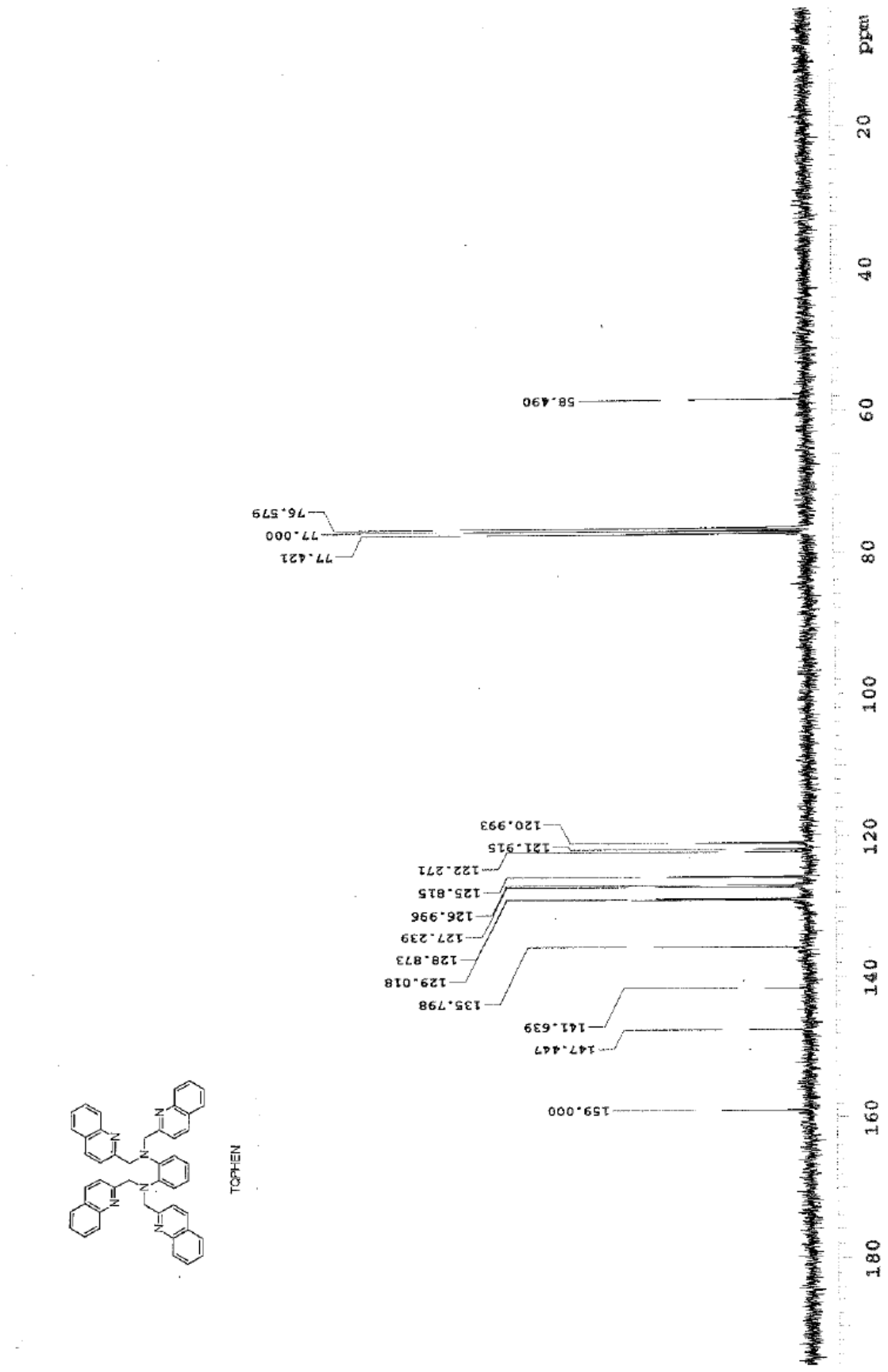

Fig. S16 ^{13}C NMR spectrum of TQPHEN in $CDCl_3$.

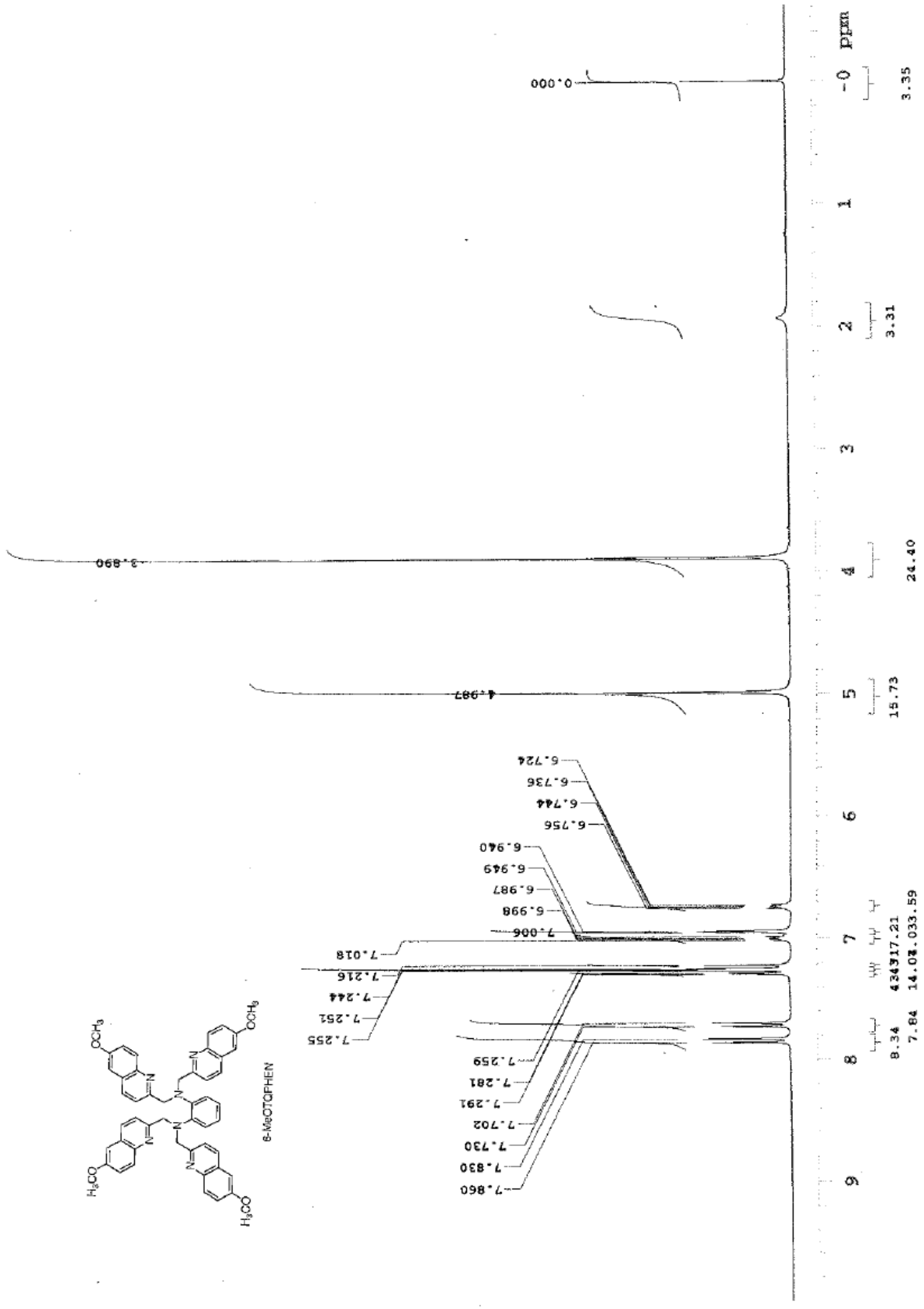

Fig. S17 ^{1}H NMR spectrum of 6-MeOTQPHEN in $CDCl_3$.

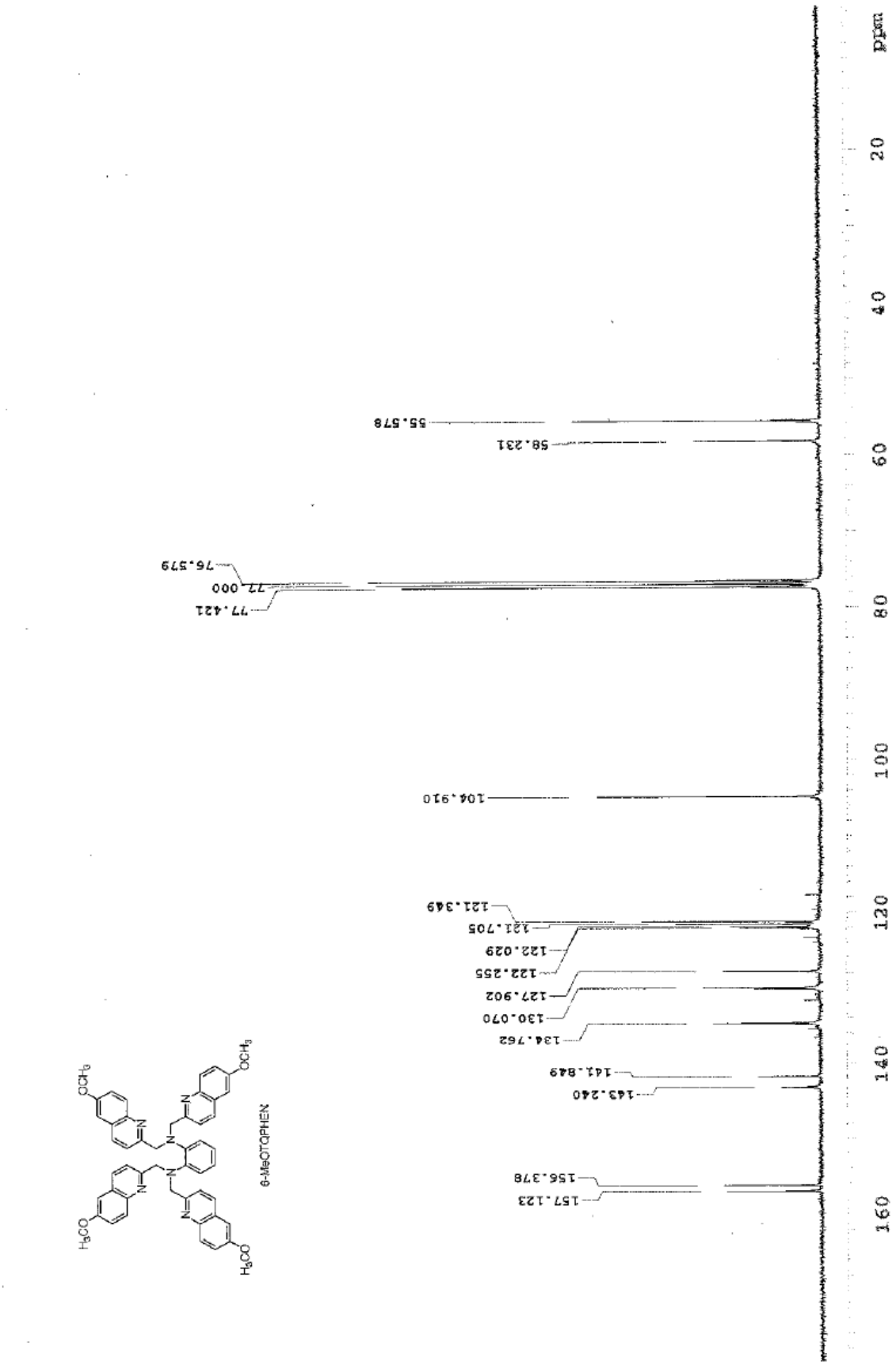

Fig. S18 ^{13}C NMR spectrum of 6-MeOTQPHEN in $CDCl_3$.

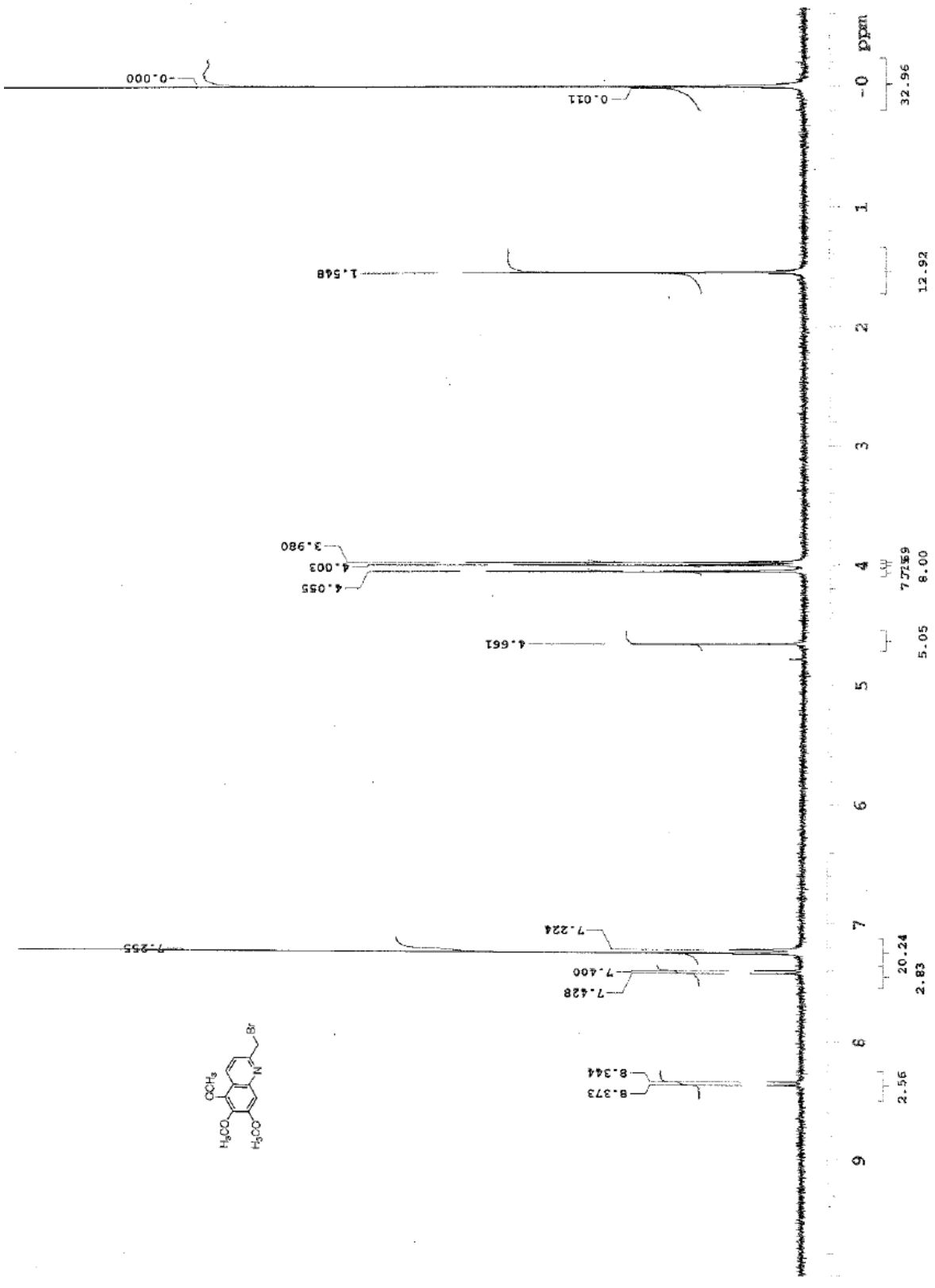

Fig. S19 ^{1}H NMR spectrum of 5,6,7-trimethoxy-2-bromomethylquinoline in $CDCl_3$.

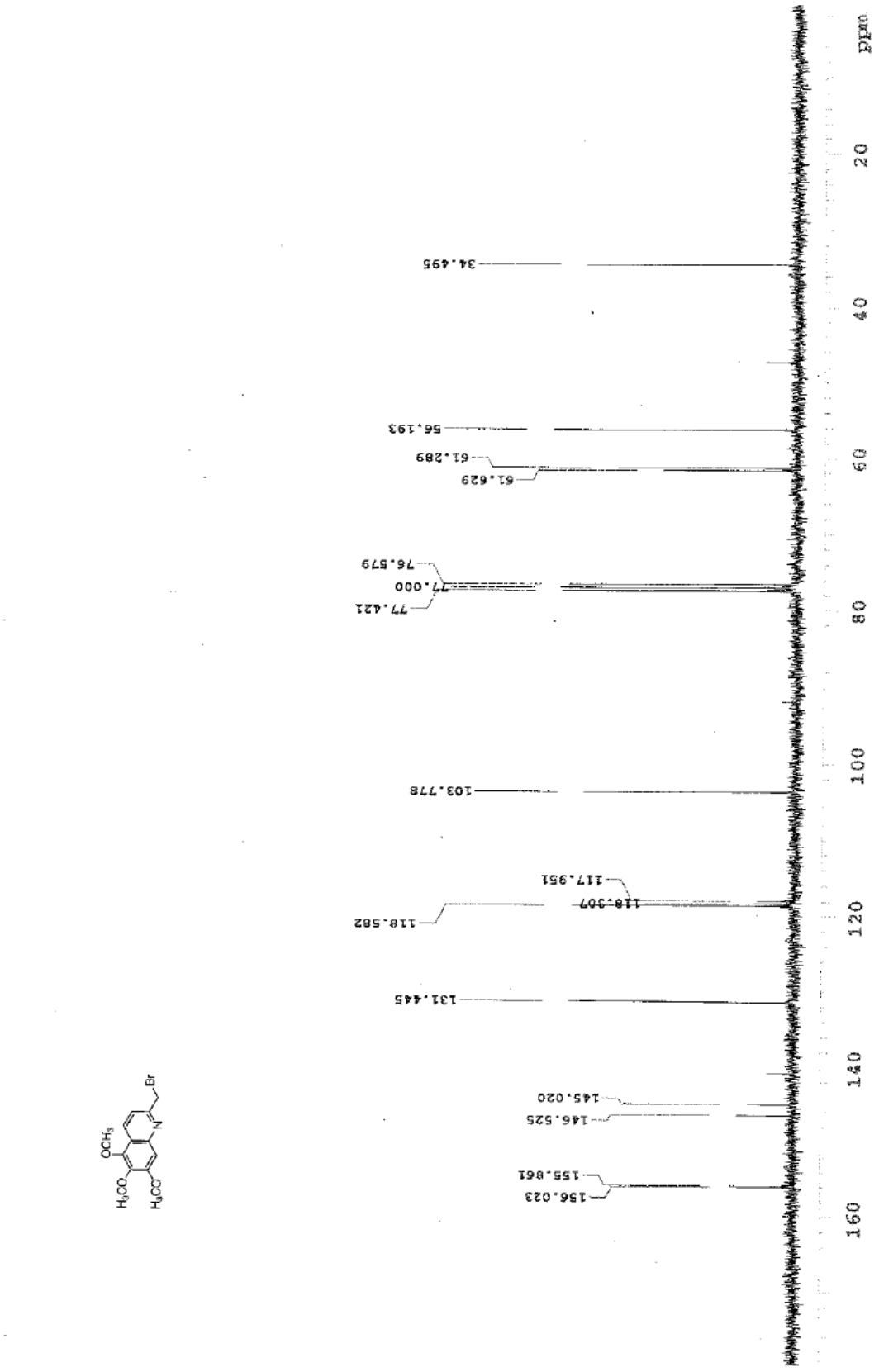

Fig. S20 ^{13}C NMR spectrum of 5,6,7-trimethoxy-2-bromomethylquinoline in $CDCl_3$.

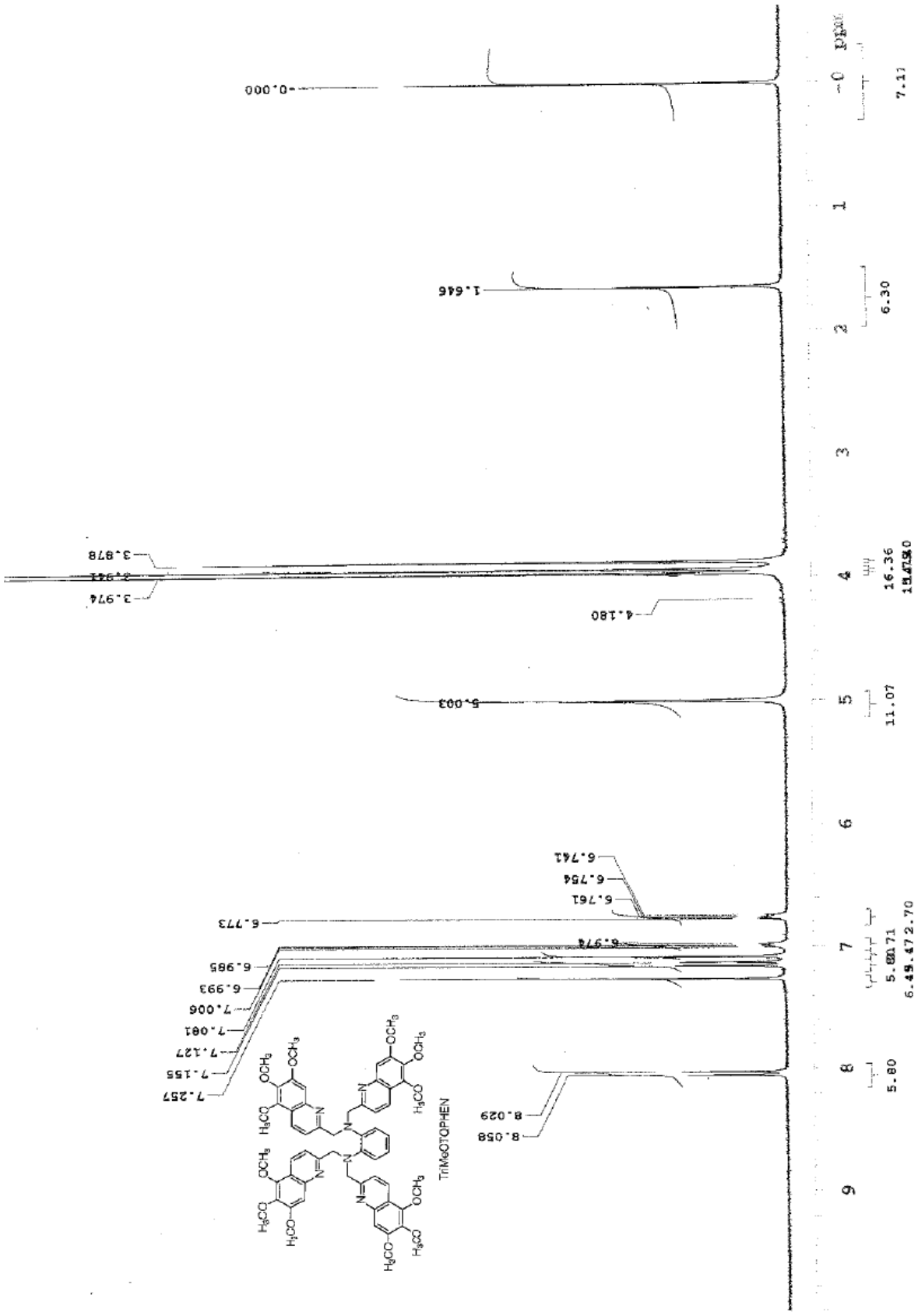

Fig. S21 ^{1}H NMR spectrum of TriMeOTQPHEN in $CDCl_3$.

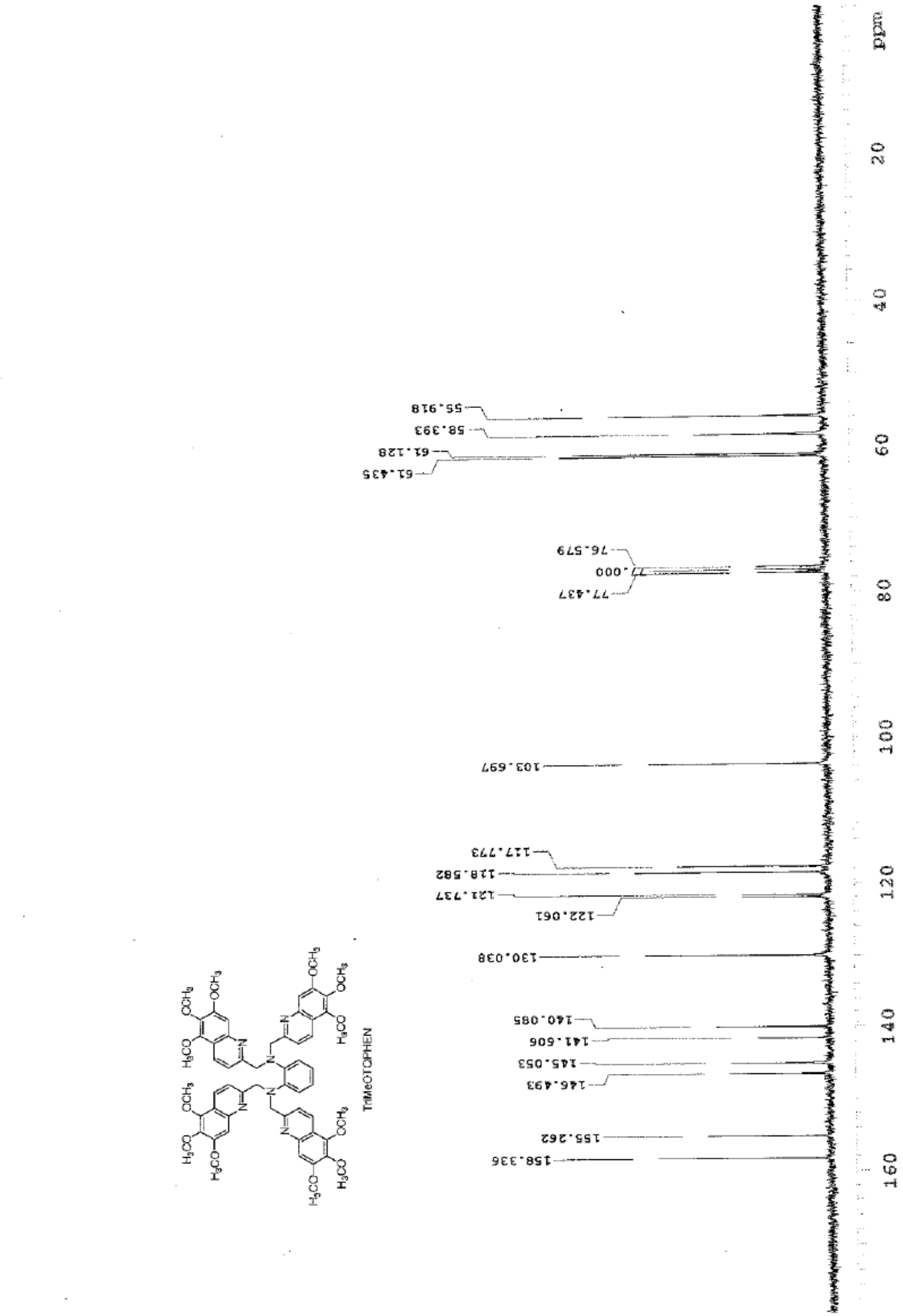

Fig. S22 ^{13}C NMR spectrum of TriMeOTQPHEN in $CDCl_3$.

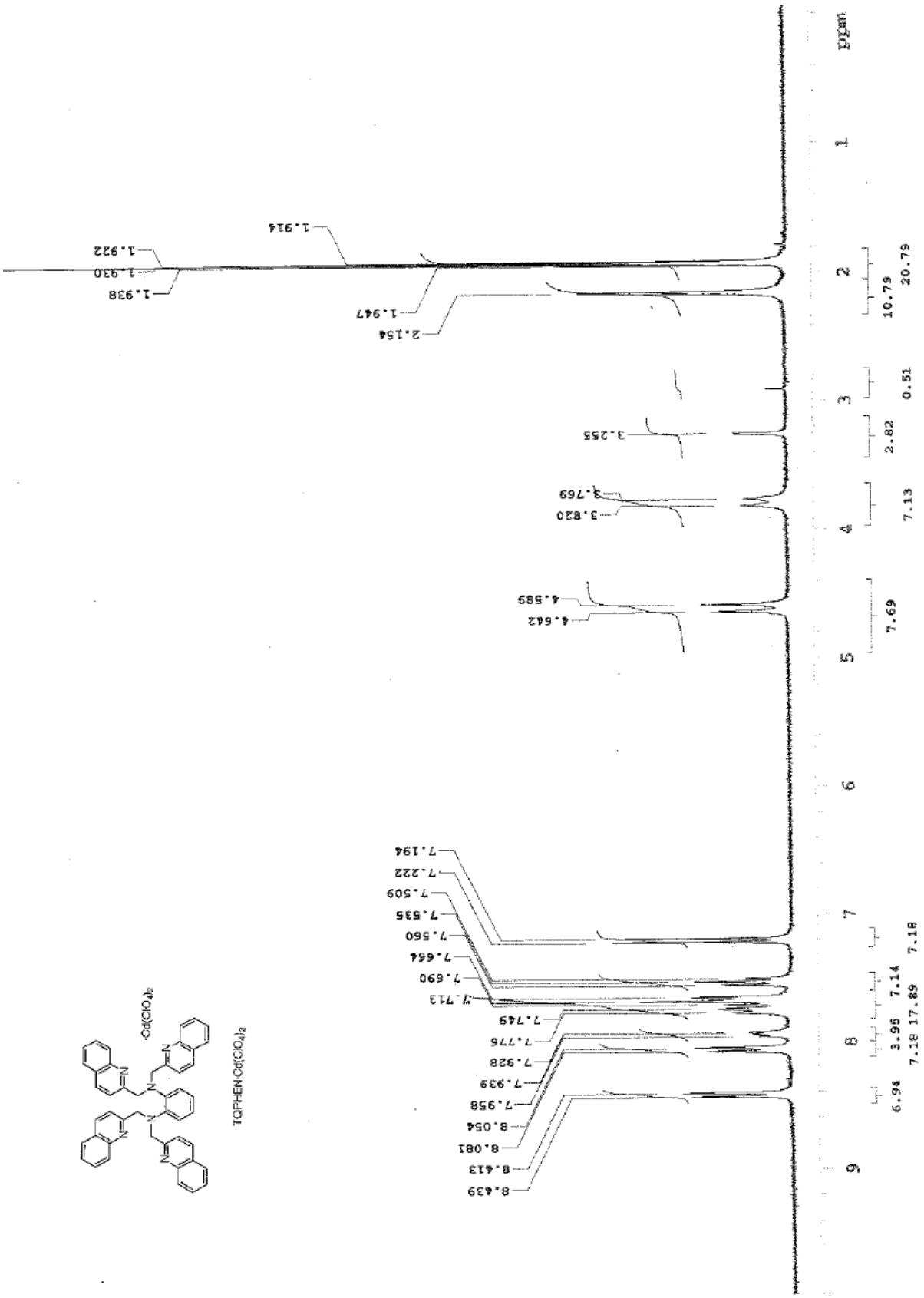

Fig. S23 ^{1}H NMR spectrum of TQPHEN·$Cd(ClO_4)_2$ in CD_3CN.

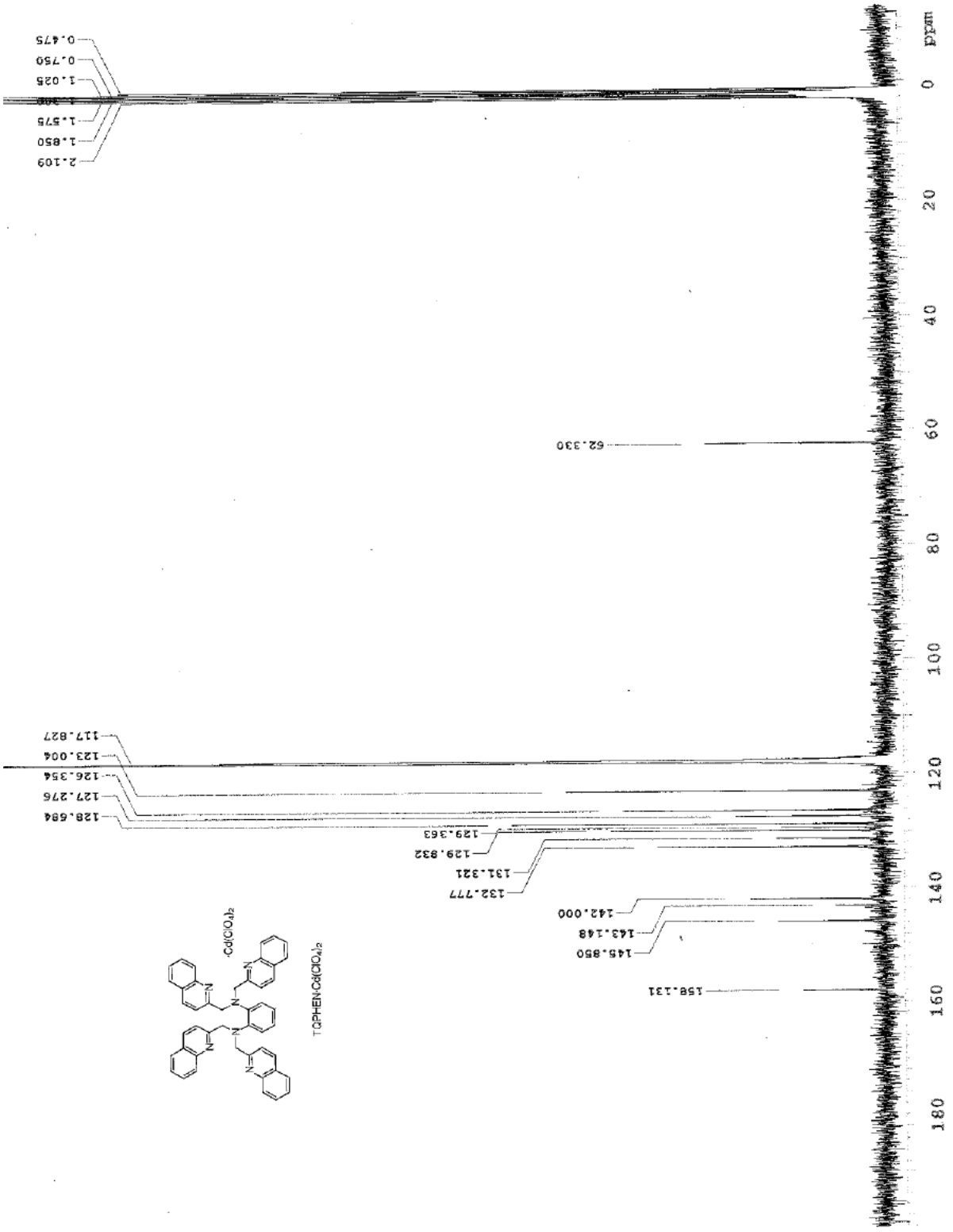

Fig. S24 ^{13}C NMR spectrum of TQPHEN·$Cd(ClO_4)_2$ in CD_3CN.

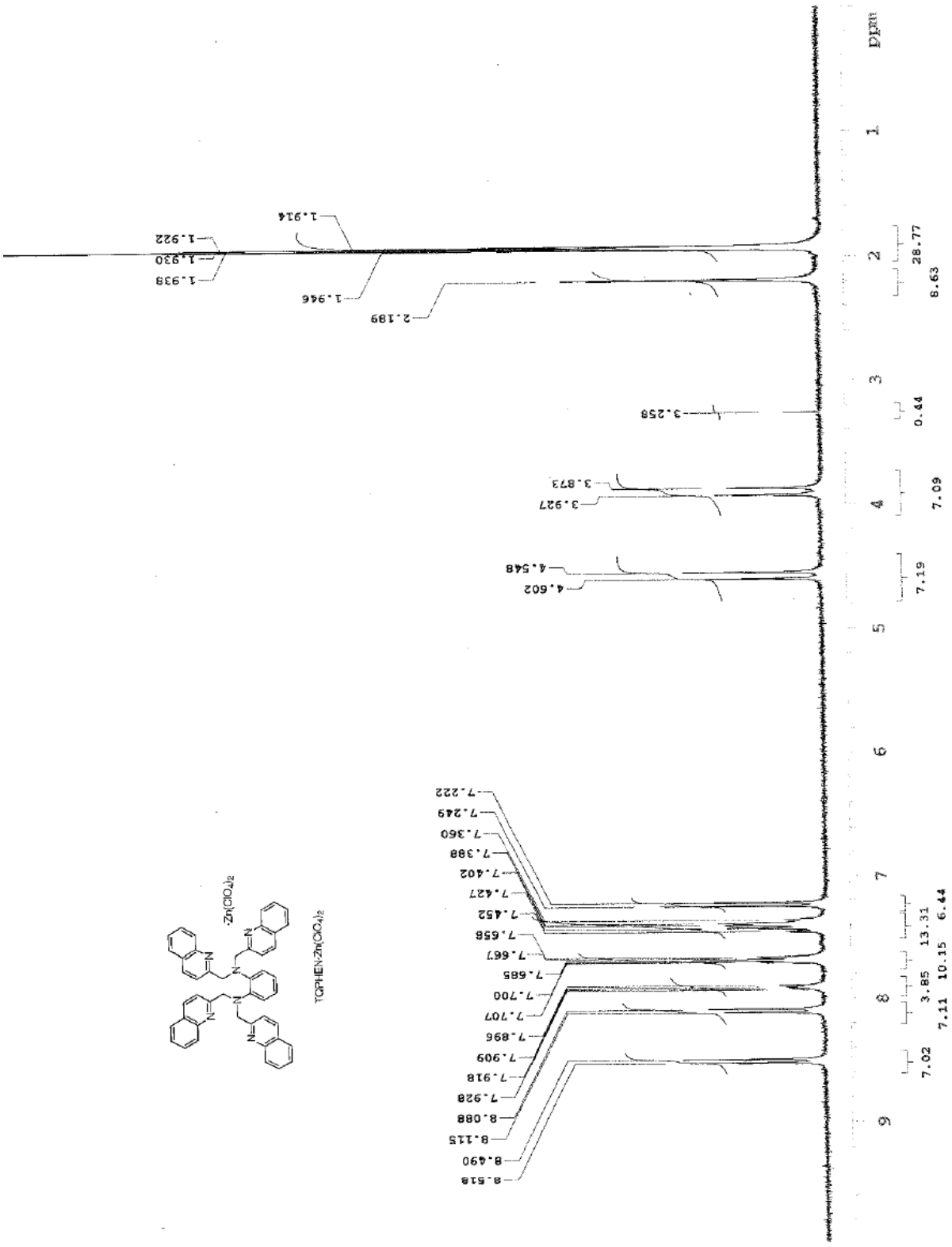

Fig. S25 ^{1}H NMR spectrum of TQPHEN·$Zn(ClO_4)_2$ in CD_3CN.

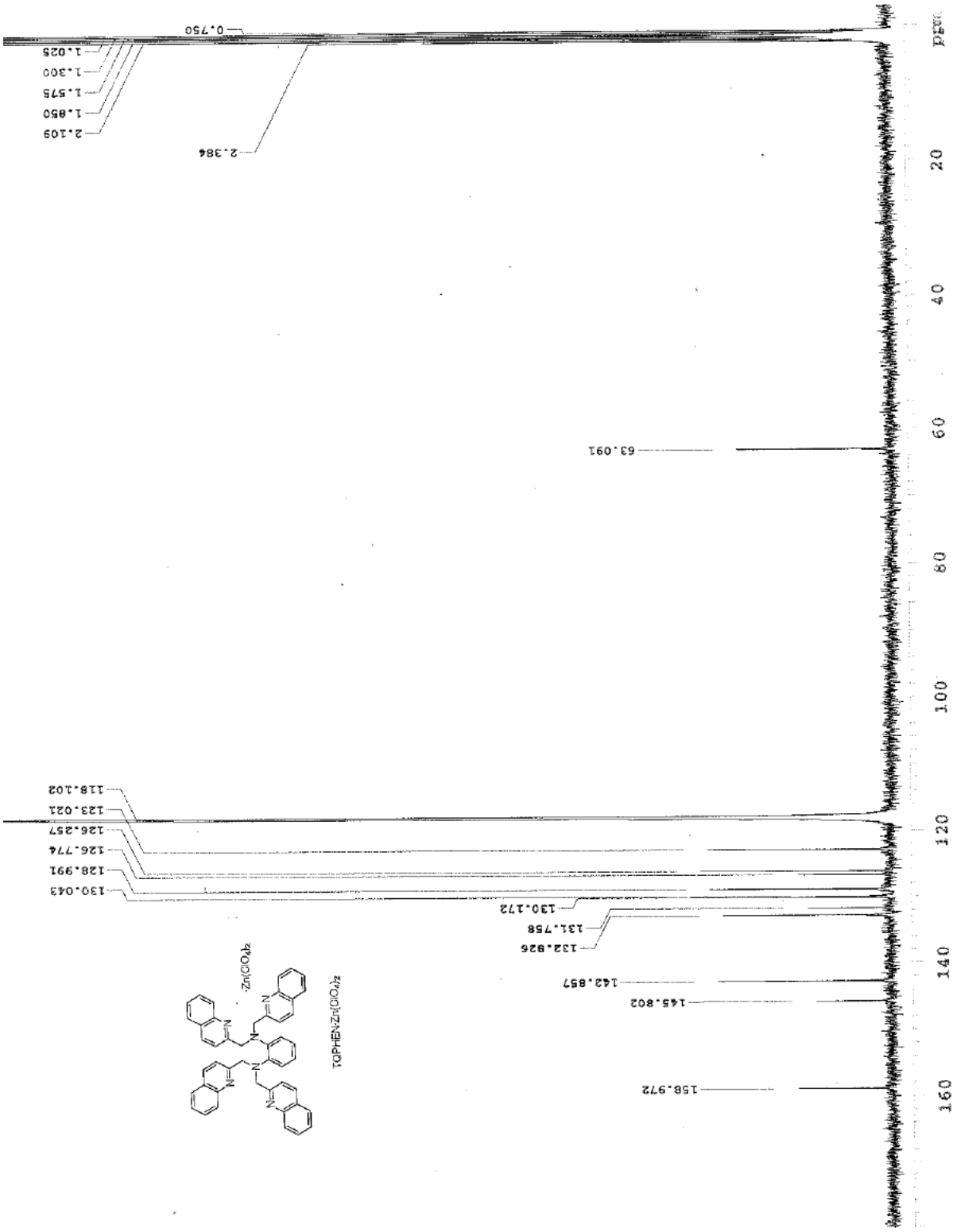

Fig. S26 ^{13}C NMR spectrum of TQPHEN·$Zn(ClO_4)_2$ in CD_3CN.